Chemical Science

ROYAL SOCIETY OF CHEMISTRY

EDGE ARTICLE

View Article Online
View Journal | View Issue

Cite this: *Chem. Sci.*, 2024, **15**, 9192

All publication charges for this article have been paid for by the Royal Society of Chemistry

Palladium-catalyzed selective C–C bond cleavage of keto-vinylidenecyclopropanes: construction of structurally rich dihydrofurans and tetrahydrofurans†

Chao Ning,[a] Ziqi Yu,[a] Min Shi *[ab] and Yin Wei *[b]

Received 17th April 2024
Accepted 14th May 2024

DOI: 10.1039/d4sc02536a

rsc.li/chemical-science

Palladium-catalyzed selective cleavage of the distal C–C bond and proximal C–C bond of keto-vinylidenecyclopropanes by altering the sterically bulky phosphine ligands has been realized. The proximal C–C bond cleavage can be achieved by using dtbpf as a phosphine ligand, affording bicyclic products containing dihydrofuran skeletons in good yields along with broad substrate scope. In proximal C–C bond cleavage reactions, the eight-membered cyclic palladium intermediate plays a key role in the reaction. The [3 + 2] cycloaddition of keto-vinylidenecyclopropanes through the distal C–C bond cleavage can be effectively accomplished with ^{t}BuXPhos as a phosphine ligand and $ZnCl_2$ as an additive, delivering bicyclic products containing tetrahydrofuran skeletons in good yields. The further transformation of these bicyclic products has been demonstrated, and the reaction mechanisms of two different C–C bond cleavage reactions have been investigated by control experiments and DFT calculations.

Introduction

Organic compounds with a bicyclic skeleton are widely found in natural products and pharmaceutical molecules.[1] In the past few decades, significant progress has been made in the construction of bicyclic compounds through transition metal (TM)-catalyzed C–C bond cleavage of alkylidenecyclopropanes (ACPs) and vinylidenecyclopropanes (VDCPs).[2,3] In the synthesis of bicyclic compounds,[4] these interesting functionalized strained small rings played key roles as three-carbon components. Particularly, several novel examples of cycloaddition reactions with regard to ACPs and VDCPs have been recently disclosed using Pd,[5] Rh,[6] Co,[7] and Ni[8] as the catalysts. For unactivated VDCPs, it has been established that oxidative addition of TM to the distal C–C bond of VDCP produces a metallacyclobutane species **I-1**, accompanied by inter- or intramolecular migratory insertion into the unsaturated C–C bond to afford metallacyclohexane species **I-2**. The metallacyclohexane species **I-2** undergoes further transformations *via* two pathways: (a) direct reductive elimination;[6e,f,i] (b) nucleophilic reagent attack,[6g,6h] furnishing the cyclized products (Scheme 1).

In the past few decades, the reaction of proximal C–C bond cleavage of alkylidenecyclopropanes has made significantly effective progress.[9] As for activated VDCPs, our group's previous work has disclosed the palladium-catalyzed and Lewis acid-assisted proximal C–C bond cleavage of the vinylidenecyclopropane-diester as shown in Scheme 2.[10] In this proximal C–C bond cleavage, a η^1-(allenyl)palladium species **II-1** is produced, which can be transformed into η^3-(propargyl)palladium species **II-2** and η^1-(propargyl)palladium species **II-3** to undergo the downstream transformations.[11] Moreover, Chen's group recently also revealed that the vinylidenecyclopropane-diester[12] reacted with nucleophilic copper species to form a vinyl copper intermediate **III-1**,[13] which underwent a β-carbo elimination to give a copper species **III-2** and a protonation to deliver products **III-3** (Scheme 2).

Thus far, the proximal C–C bond cleavage of unactivated vinylidenecyclopropane has never been reported before. As

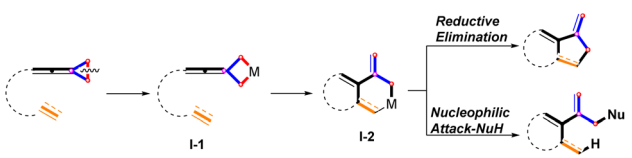

Scheme 1 TM catalyzed cycloaddition reactions of VDCPs through distal C–C bond cleavage (well-established).

[a]*Key Laboratory for Advanced Materials and Institute of Fine Chemicals, Key Laboratory for Advanced Materials and Feringa Nobel Prize Scientist Joint Research Center, School of Chemistry & Molecular Engineering, East China University of Science and Technology, Meilong Road No.130, Shanghai, 200237, China*

[b]*State Key Laboratory of Organometallic Chemistry, Center for Excellence in Molecular Synthesis, University of Chinese Academy of Sciences, Shanghai Institute of Organic Chemistry, Chinese Academy of Sciences, 345 Lingling Road, Shanghai 200032, China. E-mail: mshi@mail.sioc.ac.cn; weiyin@sioc.ac.cn*

† Electronic supplementary information (ESI) available: Experimental procedures and characterization data of new compounds. CCDC 2206931 and 2246469. For ESI and crystallographic data in CIF or other electronic format see DOI: https://doi.org/10.1039/d4sc02536a

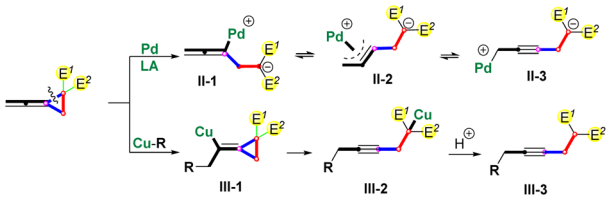

Scheme 2 Ring-opening reactions of proximal C–C bond cleavage of the VDCP-diester.

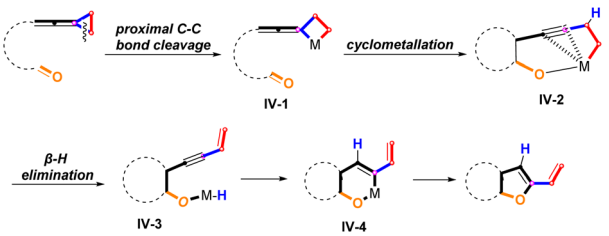

Scheme 3 Proposed ring opening reaction of proximal C–C bond cleavage of unactivated VDCP (unexplored).

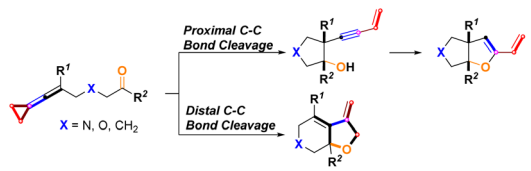

Scheme 4 This work.

a consequence, we envisaged that the activation of the proximal C–C bond of VDCPs tethered with a carbonyl group would produce a metallacyclobutane species **IV-1**, which can lead to the metallacyclic species **IV-2** through a cyclometallation process. **IV-2** is energetically and structurally stabilized by coordination of the alkyne to palladium.[14] Then, the intermediate **IV-2** undergoes a β-hydrogen elimination to generate an intermediate **IV-3**. Subsequently, intramolecular migratory insertion affords intermediate **IV-4**, which undergoes a reductive elimination to give the bicyclic product bearing a dihydrofuran skeleton (Scheme 3).[15]

In this work, we wish to report the combined results of palladium-catalyzed and sterically bulky tertiary phosphine ligand-controlled selective proximal and distal C–C bond cleavage of keto-VDCPs for the rapid construction of a series of bicyclic products containing dihydrofuran and tetrahydrofuran skeletons (Scheme 4).

Results and discussion

Experimental investigations

At the start of our investigations, keto-VDCP **1a** was used as the model substrate to examine the reaction outcomes. Interestingly, the [3 + 2] cycloaddition reactions successfully took place in the presence of 6 mol% of $Pd_2(dba)_3$ and 12 mol% of ^{t}BuXPhos in anhydrous toluene at 100 °C after 8 hours, giving **2a** in 8% isolated yield and **3a** in 46% isolated yield along with the intramolecular hydroalkoxylation product **4a** in 12% isolated yield (Table 1, entry 1). These [3 + 2] cycloaddition reactions can take place with another bulky biaryl phosphine-RuPhos, while affording the corresponding products **2a**, **3a** and **4a** in lower yields (Table 1, entry 2). Some other bisphosphine ligands including (*rac*)-BINAP were also screened, but no reaction occurred (Table 1, entries 3–5). On increasing the reaction temperature to 120 °C and increasing the amount of Pd catalyst and ^{t}BuXPhos, we found that the yield of **3a** was improved to 60% yield along with **2a** in 12% yield and **4a** in 10% yield (Table 1, entry 6). However, even under such rigorous reaction conditions, substrate **1a** still did not react completely. Inspired by Yu and Dong's work,[4i,p,q] we next considered that using $ZnCl_2$ as an additive in the catalytic system may improve the reaction outcome, and found that the yield of **3a** was considerably increased to 86% with the addition of 20 mol% $ZnCl_2$ without the formation of **2a** and **4a** (Table 1, entry 7). Furthermore, the product **3a** was exclusively obtained in 92% yield with the addition of 100 mol% $ZnCl_2$ (Table 1, entry 8). Accordingly, a series of Lewis acids were screened, such as $InCl_3$, $GaCl_3$, $Zn(OTf)_2$, $Yb(OTf)_3$ and ZnI_2, and none of them showed a better yield of the desired products than $ZnCl_2$, probably due to the good solubility of $ZnCl_2$ in toluene (Table 1, entries 9–13). The examination of solvent revealed that toluene should be used for the production of **3a** (Table 1, entries 14 and 15). Next, we tried to explore the role of K_2CO_3 in this reaction. The addition of 6 mol% $Pd_2(dba)_3$, 12 mol% ^{t}BuXPhos and 20 mol% K_2CO_3 produced **3a** in 50% yield along with **4a** in 20% yield and the result is similar to entry 1 (Table 1, entry 16). On the other hand, we also identified that the cyclized product **2a** was obtained in 80% yield along with **4a** in 12% yield using 6 mol% of $Pd_2(dba)_3$ as the catalyst and 12 mol% $HP^tBu_3BF_4$ as the ligand in the presence of 20 mol% K_2CO_3 (Table 1, entry 17). As the loading of K_2CO_3 increased to 50 mol%, the yield of product **2a** reduced to 20% and the yield of product **4a** increased to 60% in the presence of 6 mol% of $Pd_2(dba)_3$ and 12 mol% of $HP^tBu_3BF_4$ (Table 1, entry 18). Upon increasing the amount of K_2CO_3 to 100 mol%, **4a** was formed in 82% yield (Table 1, entry 19). Fortunately, the cyclized product **2a** with proximal C–C bond cleavage of **1a** was achieved in 96% yield as a sole product using dtpbf as a ligand in the absence of K_2CO_3 (Table 1, entry 20). When the reaction temperature was lowered to 90 °C, the yield of **2a** decreased to 72% (Table 1, entry 21). On adding 100 mol% K_2CO_3 into the catalytic system in the presence of 6 mol% of $Pd_2(dba)_3$ and 12 mol% of dtbpf, product **4a** becomes the major product (Table 1, entry 22). We hypothesize that a large amount of K_2CO_3 in the reaction system promotes the reductive elimination of intermediate **2-Int4** (shown in Scheme 10) more quickly than the alternative migratory insertion, affording **4a** as the major product.[16] On adding 100 mol% $ZnCl_2$ into this catalytic system, no reaction occurred (Table 1, entry 23). Solvent screening was performed and toluene was found to be the optimal solvent for this reaction as well (Table 1, entries 24–25) (for more information, see page S7 in the ESI†).

With the optimal reaction conditions established, we next explored the substrate scope of the production of **2** derived from

Table 1 Optimization of the reaction conditions[a]

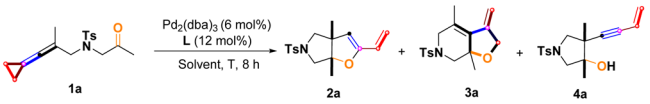

Entry[a]	Catalyst	L	Additive	Solvent	T (°C)	Yield[b]/% 2a	3a	4a
1	$Pd_2(dba)_3$	^{t}BuXPhos	None	Toluene	100	8	46	12
2	$Pd_2(dba)_3$	RuPhos	None	Toluene	100	6	26	6
3	$Pd_2(dba)_3$	dppf	None	Toluene	100	—	—	—
4	$Pd_2(dba)_3$	dppb	None	Toluene	100	—	—	—
5	$Pd_2(dba)_3$	(*rac*)-BINAP	None	Toluene	100	—	—	—
6[c]	$Pd_2(dba)_3$	^{t}BuXPhos	Nonejlv	Toluene	100	12	60	12
7	$Pd_2(dba)_3$	^{t}BuXPhos	20 mol% $ZnCl_2$	Toluene	100	—	86	Trace
8	**$Pd_2(dba)_3$**	**^{t}BuXPhos**	**100 mol% $ZnCl_2$**	**Toluene**	**100**	**—**	**96**	**Trace**
9	$Pd_2(dba)_3$	^{t}BuXPhos	100 mol% $InCI_3$	Toluene	100	—	60	Trace
10	$Pd_2(dba)_3$	^{t}BuXPhos	100 mol% $GaCI_3$	Toluene	100	—	72	Trace
11	$Pd_2(dba)_3$	^{t}BuXPhos	100 mol% $Zn(OTf)_2$	Toluene	100	—	62	Trace
12	$Pd_2(dba)_3$	^{t}BuXPhos	100 mol% $Yb(OTf)_3$	Toluene	100	—	48	Trace
13	$Pd_2(dba)_3$	^{t}BuXPhos	100 mol% ZnI_2	Toluene	100	—	82	Trace
14	$Pd_2(dba)_3$	^{t}BuXPhos	100 mol% $ZnCl_2$	Toluene	100	—	80	Trace
15	$Pd_2(dba)_3$	^{t}BuXPhos	100 mol% $ZnCl_2$	DCE	100	—	80	12
16[d]	$Pd_2(dba)_3$	^{t}BuXPhos	K_2CO_3	Toluene	100	—	50	20
17[d]	$Pd_2(dba)_3$	$HP^tBu_3BF_4$	K_2CO_3	Toluene	100	80	—	12
18[e]	$Pd_2(dba)_3$	$HP^tBu_3BF_4$	K_2CO_3	Toluene	100	20	—	60
19[f]	$Pd_2(dba)_3$	$HP^tBu_3BF_4$	K_2CO_3	Toluene	100	6	—	82
20	**$Pd_2(dba)_3$**	**dtbpf**	**None**	**Toluene**	**100**	**96**	**—**	**—**
21	$Pd_2(dba)_3$	dtbpf	None	Toluene	90	72	—	6
22[f]	$Pd_2(dba)_3$	dtbpf	K_2CO_3	Toluene	100	12	—	82
23	$Pd_2(dba)_3$	dtbpf	100 mol% $ZnCl_2$	Toluene	100	—	—	—
24	$Pd_2(dba)_3$	dtbpf	None	Dioxane	100	80	—	10
25	$Pd_2(dba)_3$	dtbpf	None	DCE	100	82	—	12

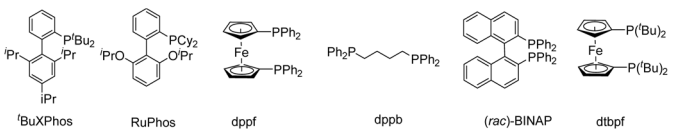

[a] Reaction conditions: substrate **1a** (0.10 mmol), $Pd_2(dba)_3$ (6 mol%) and L (12 mol%) in 1.0 mL anhydrous toluene under an argon atmosphere for 8 h. [b] Isolated yield. [c] $Pd_2(dba)_3$ (10 mol%), L (20 mol%) was added. [d] K_2CO_3 (20 mol%) was added. [e] K_2CO_3 (50 mol%) was added. [f] K_2CO_3 (100 mol%) was added.

the proximal C–C bond cleavage, and the results are summarized in Scheme 5. It can be found that R^1 can be an alkyl, cycloalkyl, or benzyl group, affording the desired products **2a–2f** in good yields ranging from 72% to 96%. The structure of **2a** was identified by X-ray diffraction, and its CIF data have been deposited in CCDC with the number 2206931. Introducing functionalized alkyl substituents such as an olefinic moiety and acetal moiety in keto-VDCPs **1** gave the desired products **2g** and **2h** in 82% yield and 93% yield, respectively. We also investigated aryl substituted **1** in this reaction and found that whether an electron-donating group, an electron-withdrawing group, or methyl substitution was introduced at different positions of the benzene ring, the reactions proceeded smoothly, giving the target products **2i–2m** in good yields ranging from 78% to 94%. 2-Naphthyl-substituted keto-VDCP **1n** was also tolerated, giving the desired product **2n** in 82% yield. We then explored the R^2 substituent in this reaction and found that R^2 can be a hydrogen atom, ethyl, and isopropyl substituents, furnishing the desired products **2o–2q** in 80% to 86% yields. In addition, R^2 can be an aromatic group as well, in which regardless of whether an electron-donating group or electron-withdrawing group was introduced at the different positions of the benzene ring, the reactions were compatible, affording the desired products **2r–2aa** in moderate to good yields ranging from 62% to 82%. Furthermore, the use of 2-naphthyl substituted and 2-thiophene substituted keto-VDCPs **1ab** and **1ac** as substrates delivered the desired products **2ab** and **2ac** in 80% yield and 36% yield, respectively. Among them oxygen atom-linked **1ad** could also be used in the reaction, giving **2ad** in 86% yield although the carbon atom-linked substrate **1ae** did not provide the corresponding product, presumably due to this substrate without the Thorpe-Ingold effect. On extending the carbon chain in the designed substrate **1af**, we found that the reaction also occurred efficiently, affording **2af** in 80% yield.

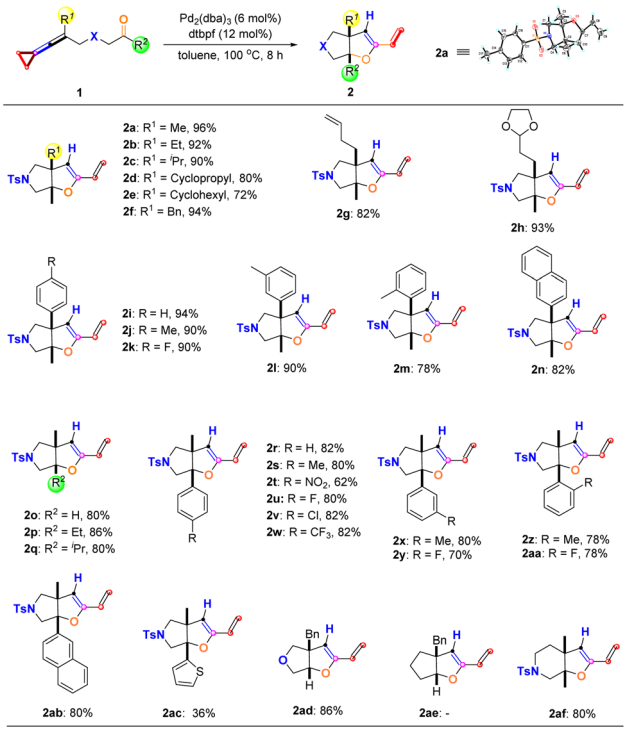

Scheme 5 Substrate scope of **2** derived from the proximal C–C bond cleavage. Reaction conditions: substrate **1** (0.10 mmol), $Pd_2(dba)_3$ (6 mol%) and dtbpf (12 mol%) in 1.0 mL anhydrous toluene under an argon atmosphere for 8 h.

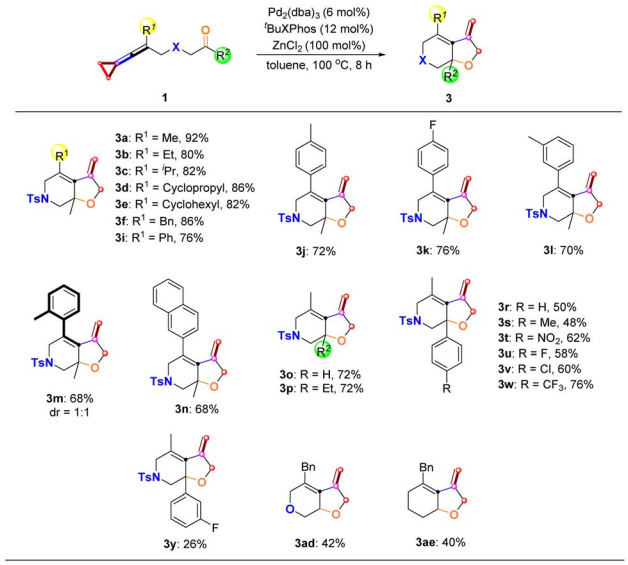

Scheme 6 Substrate scope of **3** derived from the distal C–C bond cleavage. Reaction conditions: substrate **1** (0.10 mmol), $Pd_2(dba)_3$ (6 mol%), ^{t}BuXPhos (12 mol%) and $ZnCl_2$ (100 mol%) in 1.0 mL anhydrous toluene under an argon atmosphere for 8 h.

We next explored the substrate scope for the [3 + 2] cycloaddition products **3** derived from the distal C–C bond cleavage (Scheme 6). The R^1 substituent of keto-VDCPs **1** can be an alkyl, cycloalkyl, or benzyl substituent or a phenyl group, affording the desired products **3a–3i** in 76–92% yields. A variety of electron-rich or electron-poor aryl-substituted keto-VDCPs **1** as well as naphthyl-substituted VDCP **1n** underwent this cyclization reaction smoothly, affording the corresponding products **3j–3n** in 68–76% yields. For *ortho*-methyl group substituted keto-VDCP **1m**, the desired product **3m** was a pair of atropisomers. Besides, we tried to probe the R^2 substituents of keto-VDCPs **1** and found that for the aldehyde substituted substrate **1o** and the ethyl carbonyl substituted substrate **1p**, the reactions proceeded smoothly, affording the desired products **3o** and **3p** in 72% yields, respectively. A series of electron-rich or electron-poor aryl-substituted keto-VDCPs **1r–1y** could be converted to the bicyclic products **3r–3y** in 26% to 76% yields along with a small amount of cyclized 2-chlorocyclobutene derivatives (see Scheme 8f, side effect of $ZnCl_2$). When the bridge linkage was replaced with an oxygen atom and a CH_2 moiety, the reactions were also tolerated, giving the desired products **3ad** and **3ae** in 42% yield and 40% yield, respectively.

Synthetic applications

In order to explore the synthetic applicability of these protocols, gram-scale syntheses were first performed as shown in Scheme 7a & c by employing 1.0 g (3.2 mmol) of **1a**, producing 0.9 g of **2a** in 90% yield and 0.6 g of **3a** in 60% yield, respectively under the standard conditions. Furthermore, the synthetic utilities of products **2a** and **3a** were investigated as that Pd-catalyzed hydrogenation of **2a** and **3a** furnished the corresponding reduced products **5** and **8** as diastereomeric mixtures in 96% yield and 80% yield, respectively (Scheme 7b & d). Product **2a** can be used as a dienophile and undergo a D–A cycloaddition reaction with electron deficient olefins. After screening a series of electron-deficient olefins (*e.g.*, *N*-phenylmaleimide, benzoquinone, diethyl maleate, diethyl acetylenedicarboxylate and ethene-1,1,2,2-tetracarbonitril), the product **2a** only reacted with ethene-1,1,2,2-tetracarbonitril to give the desired tricyclic product **6** in 90% yield. This reaction probably required strongly electron-deficient olefins to take place.[17] The *N*-tosyl group of **2f** was removed upon treating with sodium naphthalenide in THF at −78 °C, affording the product **7** in 90% yield (Scheme 7b). The product **3a** could be transformed into the functionalized cyclic ketone **9** in 90% yield as well as the lactone product **10** in 36% yield upon using two different oxidation methods as shown in Scheme 7d.[18,19] Removal of the *N*-tosyl group of **3f** with sodium naphthalenide afforded the isomerization product **11** in 62% yield (Scheme 7d).

Mechanistic studies

We designed and synthesized the substrate **1f′** without a cyclopropane moiety; however, the reaction of **1f′** did not occur under the standard reaction conditions. Apparently, the cyclopropane moiety plays a critical role in initiating the reaction (Scheme 8a). The control experiments indicated that **4a** could be rapidly converted to product **2a** in the presence of $Pd_2(dba)_3$ with the participation of $HP^tBu_3BF_4$ combined with K_2CO_3 (20 mol%) or ^{t}BuXPhos or dtpbf in high yields, showing that product **4a** derived from proximal C–C bond cleavage could

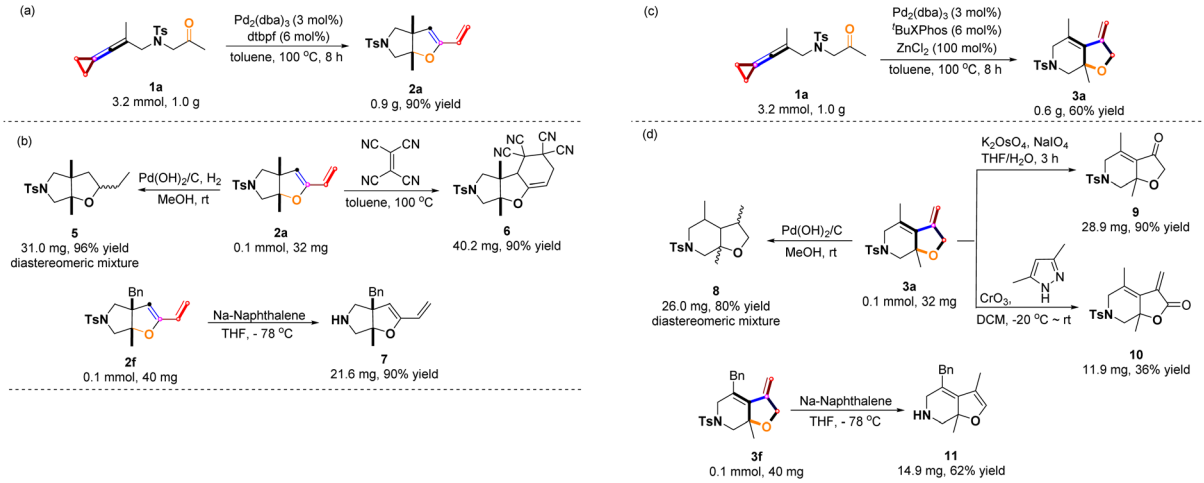

Scheme 7 Scale-up experiments and synthetic transformations: (a) Gram-scale experiment of **2a**; (b) synthetic applications of **2**; (c) Gram-scale experiment of **3a**; (d) synthetic applications of **3**.

undergo hydroalkoxylation to give the product **2a** (Scheme 8b). In addition, product **2a** cannot be converted to **3a** under the standard conditions, suggesting that products **2** and **3** are produced by their own selective C–C bond cleavages of the cyclopropane unit at the beginning of the reaction (Scheme 8c). Based on previous work, we added nucleophile like arylboronic acid and phenylacetylene in the reaction system, and attempted to obtain cross-coupled products;[5d,6e] but we only isolated the product **2a** and the unreacted substrate **1a** (for more information, see page S14 in the ESI†), probably due to intramolecular reactions taking place faster than intermolecular reactions at such a high temperature (Scheme 8d). We added 1.0 equiv of $Pd_2(dba)_3$ and 1.0 equiv of dtpbf to participate in the reaction, and product **2a** was obtained in 86% yield in 30 min. Product **2a** was also obtained in 40% yield in 10 min, and 56% of the substrate **1a** was recovered. Obviously, employing 1.0 equiv of $Pd_2(dba)_3$ and 1.0 equiv of dtpbf makes the reaction very rapid; therefore, it is difficult to obtain the reaction intermediates at such a high temperature (for more information, see page S13 in the ESI†) (Scheme 8e).

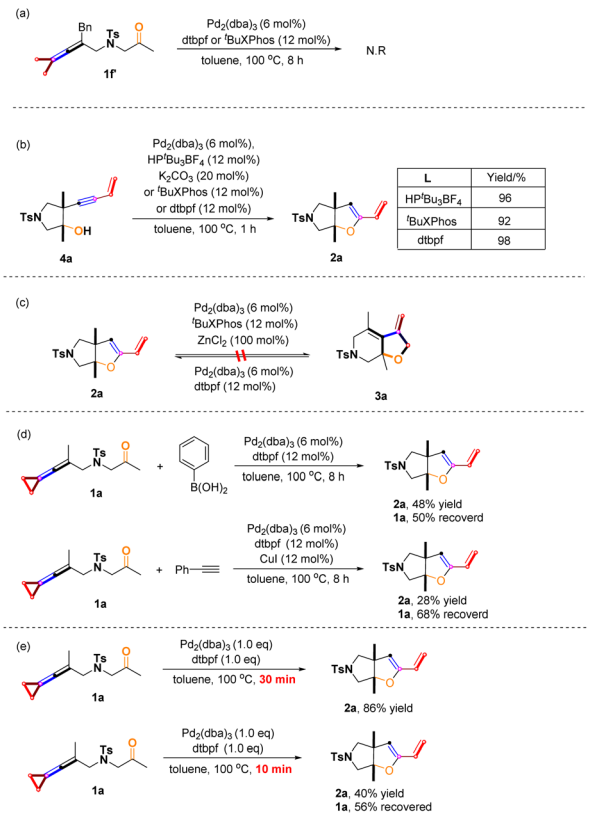

Scheme 8 Control experiments: (a) reations of **1f'** under standard conditions; (b) hydroalkoxylation of **4a** to **2a**; (c) experiments on the interconversion between **2a** and **3a**; (d) reactions of **1a** with arylboronic acids and phenylacetylene; (e) reactions under 1.0 eq. catalyst and ligand condition.

As described above, adding $ZnCl_2$ facilitated the completion of the [3 + 2] cycloaddition reaction; however, we also found that the deliquescence of $ZnCl_2$ by ambient moisture caused one side reaction, giving another cyclization product as the byproduct.[20] We attempted to explore the reaction results by adding H_2O (2.0 equiv.) under the standard conditions. The results showed that the desired [3 + 2] cycloaddition reaction and the side reaction proceeded simultaneously, affording [3 + 2] cycloaddition products **3s** and **3u** in 48% and 58% yields and the minor products **12** and **13** in 20% and 26% yields (Scheme 9a). As shown in Scheme 9b, treating **1u**, **1s** and **1ac** with $ZnCl_2$ (1.0 equiv) and water (2.0 equiv) in toluene at 100 °C provided the corresponding chlorocyclobutene derivatives **12–14** in 38–46% yields (Scheme 9b). The structure of **14** has been confirmed by X-ray diffraction and the CIF data are deposited in CCDC with the number 2246469. This finding can explain why in some cases, the [3 + 2] cycloaddition products **3** were obtained in low yields such as **3y**, **3ad**, and **3ae**.

To further understand the mechanistic paradigm, density functional theory (DFT) calculations were performed. The calculations on the tandem cyclization reaction derived from

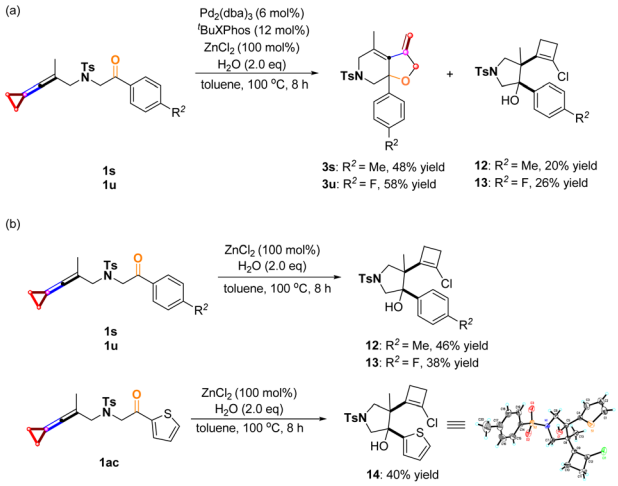

Scheme 9 (a) Reaction of adding 2.0 eq. H_2O under standard condition; side effects of aqueous $ZnCl_2$.

proximal C–C bond cleavage have been performed at the SMD(toluene)/B3LYP/6-311+G(d,p)/Lanl2dz//B3LYP/6-31G(d)/Lanl2dz level with the Gaussian 16 program. We investigated the reaction pathway starting from a stable palladium complex **2-Int1** (shown in Scheme 10a), in which the allene units of **1a** are coordinated to a palladium catalyst. The insertion of the palladium catalyst into the proximal C–C bond of VDCP produces a palladacyclic **2-Int2** through **2-Ts1** with an energy barrier of 22.4 kcal mol^{-1}. We also investigate the oxidative cyclometallation of **2-Int1** through **2-Ts1′** to generate a palladacyclic intermediate **2-Int2′**; however, this process has an extremely high energy barrier of 50.4 kcal mol^{-1}, and thus, we exclude this pathway (for more details, see Scheme S1 in page S15 of the ESI†). The intermediate **2-Int2** subsequently undergoes cyclometallation to generate an intermediate **2-Int3** *via* the transition state **2-Ts2**. The energy barrier for cyclometallation is 13.8 kcal mol^{-1}, which is lower than that of the competitive pathway involving the so-called a β-H elimination step (41.7 kcal mol^{-1} *via* **2-Ts2″**) (for more details, see Scheme

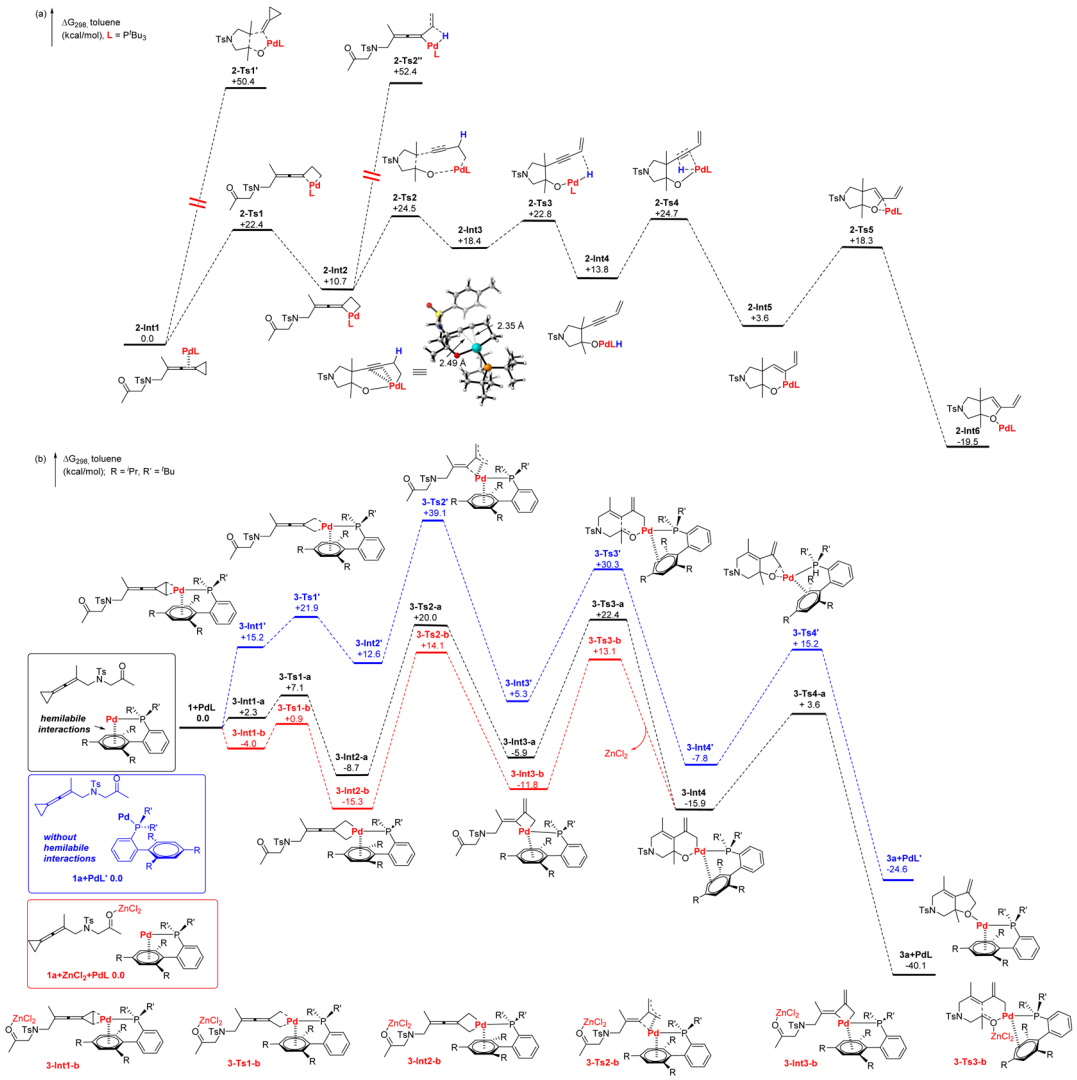

Scheme 10 DFT calculations on the possible reaction pathways: (a) DFT calculations of **1a** to **2a**; (b) DFT calculations of **1a** to **3a**.

S2 in page S16 of the ESI†). The palladium intermediates **2-Int3** presents the alkyne moiety coordinated to palladium (Pd–C≡C, 2.49 Å and 2.35 Å). The intermediate **2-Int3** is a stable intermediate, probably due to the alkyne moiety coordinated to palladium.[13] We also attempted to locate the intermediate in which the alkyne moiety is not coordinated to palladium; however, we failed to obtain such a kind of intermediate and it always reverses to the previous intermediates **2-Int1** or **2-Int2** after geometry optimization. The intermediate **2-Int3** subsequently undergoes β-hydrogen elimination to generate an intermediate **2-Int4** *via* **2-Ts3** with a low energy barrier of 4.4 kcal mol^{-1}. The intermediate **2-Int4** can undergo reductive elimination to afford product **4a**, which was accessed in the experiment. Alternatively, **2-Int4** undergoes migratory insertion *via* **2-Ts4** to generate **2-Int5** with a free energy of 10.9 kcal mol^{-1}. Subsequently, reductive elimination of **2-Int5** is performed to afford **2-Int6** *via* **2-Ts5** with an energy barrier of 14.7 kcal mol^{-1} and then releasing the palladium catalyst to form product **2a**. This is in line with the result of the control experiment shown in Scheme 8b, in which **4a** could be rapidly converted to product **2a** under standard conditions. We also investigated another possible reaction pathway that involves **2-Int2** undergoing β-C elimination followed by β-H elimination (for details, see Scheme S2 in the page S16 of ESI†).

In conjunction with the previously proposed concept of hemilabile interactions between the palladium, and bulky biaryl phosphine ligands,[5c,d] we also compared the difference between the presence and absence of hemilabile interactions by DFT calculations to show the role of the bulky biaryl phosphine ligand in the [3 + 2] cycloaddition reaction (shown in Scheme 10b). The DFT calculations for this reaction were performed at the SMD(toluene)/ωB97X-D/6-31G(d)/Lanl2dz//ωB97X-D/6-31G(d)/Lanl2dz level with the Gaussian 16 program.[21] We used the hemilabile palladium complex and substrate **1a** as the first step. The palladium complex coordinated to the distal C–C bond of VDCP to produce **3-Int1-a** with an activation free energy of 2.3 kcal mol^{-1}. The hemilabile interactions between the palladium and bulky phosphine ligands allows the energy of **3-Int1-a** to be 12.9 kcal mol^{-1} less than that of **3-Int1′**. The insertion of a palladium catalyst into the distal C–C bond of VDCP gives a palladacyclic intermediate **3-Int2-a** through **3-Ts1-a** with an energy barrier of 4.8 kcal mol^{-1}. **3-Int2-a** then isomerizes to **3-Int3-a** *via* **3-Ts2-a** with an energy barrier of 28.7 kcal mol^{-1}, which is lower than that of **3-Ts2′** due to the presence of hemilabile interactions. Subsequently, carbonyl group insertion occurs *via* **3-Ts3-a** with an activation free energy of 28.3 kcal mol^{-1} to give a palladacyclohexane intermediate **3-Int4**. Then, the reductive elimination reaction (*via* **3-Ts4**) converts **3-Int4** to **3a+PdL** with an activation free energy of 19.5 kcal mol^{-1}. For comparison, the reaction pathway without hemilabile interactions is also investigated systematically (Scheme 10b, blue letters). Generally, the energies of all intermediates and transition states without hemilabile interactions are higher in the range of 7.9–21.3 kcal mol^{-1}, indicating that hemilabile interactions play important roles in this reaction. Moreover, DFT calculations on the reaction pathway involving $ZnCl_2$-promoted the [3+2] cycloaddition were also performed (Scheme 10b, red letters). It is noteworthy that

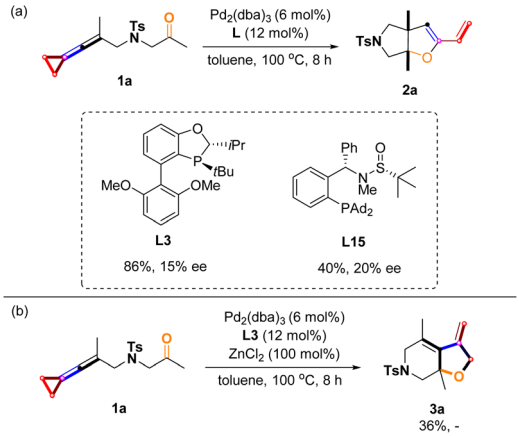

Scheme 11 (a) Asymmetric studies of **2a**; (b) asymmetric studies of **3a**.

the intermediates and transition states are more energetically stable (5.9–9.3 kcal mol^{-1}) due to binding between $ZnCl_2$ and the C=O bond in **1a**. The addition of $ZnCl_2$ decreases the energy barrier of carbonyl group insertion (**3-Int3-b** to **3-Ts3-b**) which is lower than that without $ZnCl_2$ (**3-Int3-a** to **3-Ts3-a**) by 3.4 kcal mol^{-1}, and indicates that the addition of $ZnCl_2$ facilitates the migratory insertion of the C=O bond. For comparison, the insertion of a palladium catalyst with the bulky biaryl phosphine ligand into the proximal C–C bond of VDCP which produces a palladacyclic intermediate **3-Int2-b′** was also investigated. The energy of **3-Int2-b′** is higher than that of **3-Int2-b** by 8 kcal mol^{-1}, probably due to steric hindrance. This may account for the distal C–C bond cleavage being preferred, utilizing the bulky biaryl phosphine ligand. In general, the phosphine ligand can tune the modes of the initial C–C bond cleavage, which leads to different reaction patterns and generates different products.

Asymmetric studies

The asymmetric variants of these reactions were investigated with a series of sterically bulky chiral phosphine ligands,[22,23] and we found that the use of ligands **L3** and **L15** gave **2a** in 86% yield along with 15% ee and 40% yield along with 20% ee, respectively (Scheme 11a). However, for the product **3a**, no chiral induction was observed, presumably due to the high reaction temperature (Scheme 11b) (for more information, see pages S10–S12 in the ESI†). In asymmetric catalysis, high ee values were difficult to be obtained at such a high temperature (100 °C), probably because the chiral ligands dissociate on the central palladium.

Conclusions

In summary, we have developed a divergent protocol for the palladium-catalyzed and ligand-controlled selective cleavage of the distal C–C bond and proximal C–C bond of cyclopropane units in keto-vinylidenecyclopropanes **1**, affording a series of bicyclic products containing dihydrofuran skeletons and tetrahydrofuran skeletons in moderate to good yields with a broad substrate scope and good functional group tolerance. The

further transformations of the obtained bicyclic products have been also conducted to obtain a variety of their derivatives. Control experiments and DFT calculations have been used to elucidate the reaction mechanisms of the selective C–C bond cleavage. We propose a palladium intermediate in which the alkyne moiety coordinated to palladium is the key intermediate for the reaction involving the proximal C–C bond of unactivated vinylidenecyclopropane. To the best of our knowledge, this is the first example of transition metal catalyzed cleavage of the proximal C–C bond of unactivated vinylidenecyclopropane, opening up numerous avenues for further development. The utilization of these synthetic methodologies for the synthesis of biologically active molecules is currently under investigation.

Data availability

Experimental and computational data have been made available as the ESI.†

Author contributions

C. N. contributed to the experimental work; Z. Q. Y and Y. W. contributed to the computational work. C. N., Y. W. and M. S. contributed to ideation and writing of the paper.

Conflicts of interest

There are no conflicts to declare.

Acknowledgements

We are grateful for the financial support from the National Key R & D Program of China (2023YFA1506700), the National Natural Science Foundation of China (21372250, 21121062, 21302203, 20732008, 21772037, 21772226, 21861132014, 91956115 and 22171078), Project supported by the Shanghai Municipal Science and Technology Major Project (Grant No. 2018SHZDZX03) and the Fundamental Research Funds for the Central Universities 222201717003.

References

1 (*a*) R. R. A. Kitson, A. Millemaggi and R. J. K. Taylor, *Angew. Chem. Int. Ed.*, 2009, **48**, 9426–9451; (*b*) K.-D. Umland, A. Palisse, T. T. Haug and S. F. Kirsch, *Angew. Chem., Int. Ed.*, 2011, **50**, 9965–9968; (*c*) X. Cai, W. Liang, M. Liu, X. Li and M. Dai, *J. Am. Chem. Soc.*, 2020, **142**, 13677–13682; (*d*) C. Chen, W. Cheng, J. Wang, T. Chao, M. Cheng and R. Liu, *Angew. Chem., Int. Ed.*, 2021, **60**, 4479–4484; (*e*) W. Zhang, L. Li and C.-C. Li, *Chem. Soc. Rev.*, 2021, **50**, 9430–9442.

2 (*a*) A. Brandi, S. Cicchi, F. M. Cordero and A. Goti, *Chem. Rev.*, 2003, **103**, 1213–1270; (*b*) M. Rubin, M. Rubina and V. Gevorgyan, *Chem. Rev.*, 2007, **107**, 3117–3179; (*c*) M. Shi, J.-M. Lu, Y. Wei and L.-X. Shao, *Acc. Chem. Res.*, 2012, **45**, 641–652; (*d*) D.-H. Zhang, X.-Y. Tang and M. Shi, *Acc. Chem. Res.*, 2014, **47**, 913–924.

3 (*a*) M. Shi, L.-X. Shao, J.-M. Lu, Y. Wei, K. Mizuno and H. Maeda, *Chem. Rev.*, 2010, **110**, 5883–5913; (*b*) S. Yang and M. Shi, *Acc. Chem. Res.*, 2018, **51**, 1667–1680.

4 (*a*) M. Shanmugasundaram, M.-S. Wu and C.-H. Cheng, *Org. Lett.*, 2001, **3**, 4233–4236; (*b*) E. S. Johnson, G. J. Balaich and I. P. Rothwell, *J. Am. Chem. Soc.*, 1997, **119**, 7685–7693; (*c*) T. Kawasaki, S. Saito and Y. Yamamoto, *J. Org. Chem.*, 2002, **67**, 4911–4915; (*d*) M. Shanmugasundaram, M.-S. Wu, M. Jeganmohan, C.-W. Huang and C.-H. Cheng, *J. Org. Chem.*, 2002, **67**, 7724–7729; (*e*) J. A. Varela, S. G. Rubín, C. González-Rodríguez, L. Castedo and C. Saá, *J. Am. Chem. Soc.*, 2006, **128**, 9262–9263; (*f*) T. N. Tekavec and J. Louie, *J. Org. Chem.*, 2008, **73**, 2641–2648; (*g*) A. Geny, S. Gaudrel, F. Slowinski, M. Amatore, G. Chouraqui, M. Malacria, C. Aubert and V. Gandon, *Adv. Synth. Catal.*, 2009, **351**, 271–275; (*h*) M. Gulías, A. Collado, B. Trillo, F. López, E. Oñate, M. A. Esteruelas and J. L. Mascareñas, *J. Am. Chem. Soc.*, 2011, **133**, 7660–7663; (*i*) P. Chen, T. Xu and G. Dong, *Angew. Chem., Int. Ed.*, 2014, **53**, 1674–1678; (*j*) K. Masutomi, H. Sugiyama, H. Uekusa, Y. Shibata and K. Tanaka, *Angew. Chem., Int. Ed.*, 2016, **55**, 15373–15376; (*k*) H. Ueda, K. Masutomi, Y. Shibata and K. Tanaka, *Org. Lett.*, 2017, **19**, 2913–2916; (*l*) S. Yoshizaki, Y. Shibata and K. Tanaka, *Angew. Chem., Int. Ed.*, 2017, **56**, 3590–3593; (*m*) Z. Tian, Q. Cui, C. Liu and Z. Yu, *Angew. Chem., Int. Ed.*, 2018, **57**, 15544–15548; (*n*) L. Deng, Y. Fu, S. Y. Lee, C. Wang, P. Liu and G. Dong, *J. Am. Chem. Soc.*, 2019, **141**, 16260–16265; (*o*) S.-H. Hou, X. Yu, R. Zhang, L. Deng, M. Zhang, A. Y. Prichina and G. Dong, *J. Am. Chem. Soc.*, 2020, **142**, 13180–13189; (*p*) Y. Xue and G. Dong, *J. Am. Chem. Soc.*, 2021, **143**, 8272–8277; (*q*) G.-Y. Zhang, P. Zhang, B.-W. Li, K. Liu, J. Li and Z.-X. Yu, *J. Am. Chem. Soc.*, 2022, **144**, 21457–21469; (*r*) S.-H. Hou, X. Yu, R. Zhang, C. Wagner and G. Dong, *J. Am. Chem. Soc.*, 2022, **144**, 22159–22169.

5 (*a*) I. Nakamura, B. H. Oh, S. Saito and Y. Yamamoto, *Angew. Chem., Int. Ed.*, 2001, **40**, 1298–1300; (*b*) F. Verdugo, L. Villarino, J. Durán, M. Gulías, J. L. Mascareñas and F. López, *ACS Catal.*, 2018, **8**, 6100–6105; (*c*) F. Verdugo, E. Da Concepción, R. Rodiño, M. Calvelo, J. L. Mascareñas and F. López, *ACS Catal.*, 2020, **10**, 7710–7718; (*d*) F. Verdugo, R. Rodiño, M. Calvelo, J. L. Mascareñas and F. López, *Angew. Chem., Int. Ed.*, 2022, **61**, e20220229; (*e*) J. Zhou, L. Meng, S. Lin, B. Cai and J. Joelle Wang, *Angew. Chem., Int. Ed.*, 2023, **62**, e202303727.

6 (*a*) P. A. Evans and P. A. Inglesby, *J. Am. Chem. Soc.*, 2008, **130**, 12838–12839; (*b*) S. Mazumder, D. Shang, D. E. Negru, M.-H. Baik and P. A. Evans, *J. Am. Chem. Soc.*, 2012, **134**, 20569–20572; (*c*) P. A. Inglesby, J. Bacsa, D. E. Negru and P. A. Evans, *Angew. Chem., Int. Ed.*, 2014, **53**, 3952–3956; (*d*) P. A. Evans, D. E. Negru and D. Shang, *Angew. Chem., Int. Ed.*, 2015, **54**, 4768–4772; (*e*) S. Yang, K.-H. Rui, X.-Y. Tang, Q. Xu and M. Shi, *J. Am. Chem. Soc.*, 2017, **139**, 5957–5964; (*f*) S. Yang, Q.-Z. Li, C. Xu, Q. Xu and M. Shi, *Chem. Sci.*, 2018, **9**, 5074–5081; (*g*) K.-H. Rui, S. Yang, Y. Wei and M. Shi, *Org. Chem. Front.*, 2019, **6**, 2506–2513; (*h*) K.-H. Rui and M. Shi, *Org. Chem. Front.*, 2019, **6**, 1816–1820; (*i*)

X. Chen, C. Ning, S. Yang, Y. Wei and M. Shi, *Adv. Synth. Catal.*, 2021, **363**, 1727–1732.

7 (*a*) E. Da Concepción, I. Fernández, J. L. Mascareñas and F. López, *Angew. Chem., Int. Ed.*, 2021, **60**, 8182–8188; (*b*) X. Xiao and Z. Yu, *Chem.–Eur. J.*, 2021, **27**, 7176–7182.

8 (*a*) S. Saito, M. Masuda and S. Komagawa, *J. Am. Chem. Soc.*, 2004, **126**, 10540–10541; (*b*) S. Komagawa and S. Saito, *Angew. Chem., Int. Ed.*, 2006, **45**, 2446–2449; (*c*) L. Saya, G. Bhargava, M. A. Navarro, M. Gulías, F. López, I. Fernández, L. Castedo and J. L. Mascareñas, *Angew. Chem., Int. Ed.*, 2010, **49**, 9886–9890; (*d*) S. Saito, K. Maeda, R. Yamasaki, T. Kitamura, M. Nakagawa, K. Kato, I. Azumaya and H. Masu, *Angew. Chem., Int. Ed.*, 2010, **49**, 1830–1833; (*e*) L. Saya, I. Fernández, F. López and J. L. Mascareñas, *Org. Lett.*, 2014, **16**, 5008–5011.

9 (*a*) L.-Z. Yu, K. Chen, Z.-Z. Zhu and M. Shi, *Chem. Commun.*, 2017, **53**, 5935–5945; (*b*) L. Yu and M. Shi, *Chem.–Eur. J.*, 2019, **25**, 7591–7606; (*c*) H.-S. Li, S.-C. Lu, Z.-X. Chang, L. Hao, F.-R. Li and C. Xia, *Org. Lett.*, 2020, **22**, 5145–5150; (*d*) Z. Shen, I. Maksso, R. Kuniyil, T. Rogge and L. Ackermann, *Chem. Commun.*, 2021, **57**, 3668–3671; (*e*) X.-L. Liu, Y.-Y. Zhang, L. Li, L.-Q. Tan, Y.-A. Huang, A.-J. Ma and J.-B. Peng, *Org. Lett.*, 2022, **24**, 6692–6696; (*f*) M.-M. Ji, P.-R. Liu, J.-D. Yan, Y.-Y. He, H. Li, A.-J. Ma and J.-B. Peng, *Org. Lett.*, 2024, **26**, 231–235.

10 (*a*) B. Niu, Y. Wei and M. Shi, *Chem. Commun.*, 2021, **57**, 4783–4786; (*b*) Z. Yang, B. Zhang, Y. Long and M. Shi, *Chem. Commun.*, 2022, **58**, 9926–9929; (*c*) B. Wu, Q.-J. Ding, Z.-L. Wang and R. Zhu, *J. Am. Chem. Soc.*, 2023, **145**, 2045–2051.

11 (*a*) K. Tsutsumi, S. Ogoshi, S. Nishiguchi and H. Kurosawa, *J. Am. Chem. Soc.*, 1998, **120**, 1938–1939; (*b*) T. Murahashi, S. Ogoshi and H. Kurosawa, *Chem. Rec.*, 2003, **3**, 101–111.

12 (*a*) J. Chen, S. Gao and M. Chen, *Chem. Sci.*, 2019, **10**, 10601–10606; (*b*) J. Chen, S. Gao and M. Chen, *Org. Lett.*, 2019, **21**, 8800–8804; (*c*) M. Chen, *Chem. Commun.*, 2021, **57**, 9212–9215.

13 W. Yuan, L. Song and S. Ma, *Angew. Chem., Int. Ed.*, 2016, **55**, 3140–3143.

14 (*a*) Y. Yamamoto, A. Nagata, Y. Arikawa, K. Tatsumi and K. Itoh, *Organometallics*, 2000, **19**, 2403–2405; (*b*) Y. Yamamoto, A. Nagata, H. Nagata, Y. Ando, Y. Arikawa, K. Tatsumi and K. Itoh, *Chem.–Eur. J.*, 2003, **9**, 2469–2483; (*c*) Y. Yamamoto, S. Kuwabara, Y. Ando, H. Nagata, H. Nishiyama and K. Itoh, *J. Org. Chem.*, 2004, **69**, 6697–6705; (*d*) X. Lian and S. Ma, *Angew. Chem., Int. Ed.*, 2008, **47**, 8255–8258; (*e*) Y. Feng, N. Tian, Y. Li, C. Jia, X. Li, L. Wang and X. Cui, *Org. Lett.*, 2017, **19**, 1658–1661; (*f*) H. Miura, Y. Tanaka, K. Nakahara, Y. Hachiya, K. Endo and T. Shishido, *Angew. Chem., Int. Ed.*, 2018, **57**, 6136–6140.

15 (*a*) R. M. P. Veenboer, S. Dupuy and S. P. Nolan, *ACS Catal.*, 2015, **5**, 1330–1334; (*b*) Q. Li, X. Fang, R. Pan, H. Yao and A. Lin, *J. Am. Chem. Soc.*, 2022, **144**, 11364–11376; (*c*) Q. He, L. Zhu, Z.-H. Yang, B. Zhu, Q. Ouyang, W. Du and Y.-C. Chen, *J. Am. Chem. Soc.*, 2021, **143**, 17989–17994.

16 (*a*) S.-C. Sha, J. Zhang and P. J. Walsh, *Org. Lett.*, 2015, **17**, 410–413; (*b*) H. Zhang, P. Ruiz-Castillo and S. L. Buchwald, *Org. Lett.*, 2018, **20**, 1580–1583; (*c*) P.-X. Zhou, X. Yang, X. Du, S. Zhao, H. Wang, X. Li, N. Liu, X. Tan, F. Ren and Y.-M. Liang, *Org. Chem. Front.*, 2022, **9**, 4097–4103; (*d*) S. Yu, Y. Ai, L. Hu, G. Lu, C. Duan and Y. Ma, *Angew. Chem., Int. Ed.*, 2022, **61**, e202200052.

17 (*a*) D. L. Boger and C. E. Brotherton, *J. Am. Chem. Soc.*, 1986, **108**, 6695–6713; (*b*) M. H. Cheng, *J. Chem. Soc., Chem. Commun.*, 1992, 934–936.

18 W. G. Salmond, M. A. Barta and J. L. Havens, *J. Org. Chem.*, 1978, **43**, 2057–2059.

19 R. Pappo, D. Allen Jr, R. Lemieux and W. Johnson, *J. Org. Chem.*, 1956, **21**, 478–479.

20 (*a*) T. Xu, Z. Yu and L. Wang, *Org. Lett.*, 2009, **11**, 2113–2116; (*b*) T. Xu, Q. Yang, D. Li, J. Dong, Z. Yu and Y. Li, *Chem.–Eur. J.*, 2010, **16**, 9264–9272; (*c*) S. Yang, W. Yuan, Q. Xu and M. Shi, *Chem.–Eur. J.*, 2015, **21**, 15964–15969.

21 For ωB97X-D functional, see: J.-D. Chai and M. Head-Gordon, Long-range corrected hybrid density functionals with damped atom–atom dispersion corrections, *Phys. Chem. Chem. Phys.*, 2008, **10**, 6615–6620.

22 (*a*) G. Xu, C. H. Senanayake and W. Tang, *Acc. Chem. Res.*, 2019, **52**, 1101–1112; (*b*) H. Yang and W. Tang, *Chem. Rec.*, 2020, **20**, 23–40; (*c*) H. Yang and W. Tang, *Nat. Commun.*, 2022, **13**, 4577.

23 (*a*) Y. Tu, B. Xu, Q. Wang, H. Dong, Z.-M. Zhang and J. Zhang, *J. Am. Chem. Soc.*, 2023, **145**, 4378–4383; (*b*) S. Zhang, S. Wu, Q. Wang, S. Xu, Y. Han, C. Yan, J. Zhang and L. Wang, *Angew. Chem., Int. Ed.*, 2023, **62**, e202300309.